Sensors and Actuators B 255 (2018) 1254–1261

Contents lists available at ScienceDirect

Sensors and Actuators B: Chemical

journal homepage: www.elsevier.com/locate/snb

Cobalt nitride nanowire array as an efficient electrochemical sensor for glucose and H_2O_2 detection

Fengyu Xie [a,b,*,1], Xiaoqin Cao [b,c,1], Fengli Qu [d], Abdullah M. Asiri [e], Xuping Sun [b,*]

[a] College of Chemistry and Materials Science, Sichuan Normal University, Chengdu 610068, Sichuan, China
[b] Chemical Synthesis and Pollution Control, Key Laboratory of Sichuan Province, School of Chemistry and Chemical Engineering, China West Normal University, Nanchong 637002, Sichuan, China
[c] College of Life Science and Engineering, Southwest Jiaotong University, Chengdu 610031, Sichuan, China
[d] College of Chemistry and Chemical Engineering, Qufu Normal University, Qufu 273165, Shandong, China
[e] College of Chemical and Environmental Department, Faculty of Science, King Abdulaziz University, Jeddah 21589, Saudi Arabia

ARTICLE INFO

Article history:
Received 3 April 2017
Received in revised form 25 July 2017
Accepted 11 August 2017
Available online 18 August 2017

Keywords:
Cobalt nitride nanowire
Non-enzymatic
Glucose
H_2O_2
Amperometric sensor

ABSTRACT

It is highly attractive to develop non-noble-metal nanoarray architecture as a high-active catalyst electrode for molecular detection due to its large specific surface area and easy accessibility to target molecules. In this paper, we demonstrate the development of cobalt nitride nanowire array on Ti mesh (Co_3N NW/TM) as an efficient catalyst electrode for glucose oxidation in alkaline solutions and H_2O_2 reduction in neutral solutions. Electrochemical tests suggest that such Co_3N NW/TM possesses superior non-enzymatic sensing ability toward rapid glucose and H_2O_2 detection. As a glucose sensor, this fabricated electrode offers a high sensitivity of 3325.6 μA mM^{-1} cm^{-2}, with a wide linear range from 0.1 μM to 2.5 mM, a low detection limit of 50 nM (S/N = 3), and satisfactory stability and reproducibility. Its application in determining glucose in human blood serum is also successful. Amperometric H_2O_2 sensing can also been realized with a sensitivity of 139.9 μA mM^{-1} cm^{-2}, a linear range from 2 μM to 28 mM, and a detection limit of 1 μM (S/N = 3). This nanoarray architecture holds great promise as an attractive sensing platform toward electrochemical small molecules detection.

© 2017 Published by Elsevier B.V.

1. Introduction

Glucose is a source of energy for daily activities of the human body, while an excess amount of glucose in blood could lead to many endocrine metabolic diseases such as diabetes, which is one of the serious diseases causing death and disability in the world [1]. Therefore, it is highly attractive to develop accurate and convenient method for glucose sensing in clinic diagnose of diabetes. In fact, the past several years have witnessed the establishment of several sensing technologies based on magnetic [2–6]. Among them, electrochemical sensing techniques received more attention during to their fast response, easy fabrication, and miniaturized equipment. The first enzyme-based glucose biosensor was reported by Clark and Lyons in 1962 [7], and so far, commercial glucose sensors are mainly based on glucose oxidase-assisted glucose electro-oxidation. Despite with high sensitivity and selectivity, such sensor suffers from high cost, low reproducibility, complex and tedious enzyme immobilization process, and degradation of activity [8], limiting their large-scale applications. To avoid such issues, much effort has been put into designing and exploiting non-enzymatic sensors based on direct electrocatalysis of electrode materials [9].

Co is an interesting transition metal with catalytic activity toward electrocatalysis of glucose oxidation. In recent years, various Co-based catalysts with different oxidation states, shapes, and supports have been reported for non-enzymatic glucose sensing, including $Co(OH)_2$, CoOOH, and Co_3O_4, etc. [10–13]. However, all these catalyst suffer from poor conductivity, which is not beneficial to enhanced electrochemical performances. To achieve more efficient electrocatalysis, the catalyst electrode is required with improved conductivity for facilitated electron transfer and a large surface area for more exposed active sites and more contacted target analytes [14–16]. Nanoarray catalyst directly grown on current collector would be an ideal such candidate. In contrast, cobalt nitride, a class of transition metal nitrides (TMNs), possesses supe-

* Corresponding authors at: Chemical Synthesis and Pollution Control, Key Laboratory of Sichuan Province, School of Chemistry and Chemical Engineering, China West Normal University, Nanchong 637002, Sichuan, China.
E-mail addresses: xie.fengyu@hotmail.com (F. Xie), sunxp@cwnu.edu.cn (X. Sun).
[1] F. Xie and X. Cao contributed equally to this work.

http://dx.doi.org/10.1016/j.snb.2017.08.098
0925-4005/© 2017 Published by Elsevier B.V.

rior electric conductivity [17]. It is thus expected that such cobalt nitride nanoarray could exhibit superior sensing performance for non-enzymatic glucose sensing, which, however, has not been addressed before.

In this paper, we report on the development of cobalt nitride nanowire array on Ti mesh (Co_3N NW/TM) via NH_3 nitridation from $Co(CO_3)_{0.5}(OH)\cdot 0.11H_2O$ as a high-active catalyst electrode for glucose oxidation in alkaline media. As a non-enzymatic glucose sensor, this Co_3N NW/TM electrode exhibits superior sensing performances with a short response time of less than 5 s, a wide detection range of 0.1 μM to 2.5 mM, a low detection limit of 50 nM (S/N = 3), and a response sensitivity of 3325.6 $\mu A\,mM^{-1}\,cm^{-2}$, with satisfactory selectivity and reproducibility, and efficient for glucose detection in human blood serum. Obviously, it is also have response to catalyze H_2O_2 reduction in 0.1 M PBS (pH = 7.4), behaving as an electrochemical H_2O_2 sensor with a linear range from 2 μM to 28 mM, a detection limit of 1 μM (S/N = 3), and a sensitivity of 139.9 $\mu A\,mM^{-1}\,cm^{-2}$.

2. Experimental

2.1. Reagents and materials

NH_4F, lactose, urea, fructose, galactose and glucose were purchased from Beijing Chemical Works. Cobalt nitrate hexahydrate ($Co(NO_3)_2\cdot 6H_2O$), sodium hydroxide (NaOH), sodium chloride (NaCl), ascorbic acid (AA), uric acid (UA) and dopamine (DA) were purchased from Aladdin Ltd. (Shanghai, China). $K_2HPO_4\cdot 3H_2O$, $KH_2PO_4\cdot 3H_2O$ and H_2O_2 were purchased from Chengdu kelon reagent Co., Ltd. All reagents were used as received without further purification. Titanium mesh (TM) was provided by Hongshan District, Wuhan Instrument Surgical Instruments business and was cleaned by sonication sequentially in acetone, water and ethanol several times to remove the surface impurities. Ultrapure water was utilized to prepare all solutions.

2.2. Preparation of $Co(CO_3)_{0.5}(OH).0.11H_2O$ NW/TM and Co_3N NW/TM

Before experiment, TM was washed with HCl, ethanol, and water several times to remove the surface impurities. $Co(CO_3)_{0.5}(OH).0.11H_2O$ was prepared according to the previous reported as follows [14], $Co(NO_3)_2\cdot 6H_2O$ (0.291 g), NH_4F (0.093 g) and urea (0.30 g) were dissolved in 20 mL water under vigorous stirring for 30 min. Then the solution was transferred into a Teflon-lined stainless autoclave (40 mL) and a piece of TM (3 cm × 2 cm) was immersed into the solution. The autoclave was sealed and maintained at 120 °C for 6 h in an electric oven. After the autoclave cooled down slowly at room temperature, the $Co(CO_3)_{0.5}(OH).0.11H_2O$ was taken out and washed with water thoroughly before vacuum dried. To make Co_3N NW/TM, $Co(CO_3)_{0.5}(OH).0.11H_2O$ was placed in the furnace and heated to 380 °C with a heating speed of 5 °C min^{-1} under a flowing NH_3 atmosphere. After reacting 3 h at 380 °C, the system was allowed to cool down to room temperature naturally still under a flowing NH_3 atmosphere. Finally, the gray Co_3N NW/TM was collected for further characterization. We calculate the loading for Co_3N on TM using the following equation: loading = F/A, where F is the difference between the TM with and without Co_3N NW; A is the geometric area of TM (0.25 cm^{-2}). The loading for Co_3N on TM was determined to be 1.21 mg cm^{-2}.

2.3. Characterization

X-ray diffraction (XRD) data were collected on a RigakuD/MAX 2550 diffractometer with Cu Kα radiation (λ = 1.5418 Å). Scanning electron microscopy (SEM) measurements were carried out on a HITACHI S-4800 field emission scanning electron microscope at an accelerating voltage of 20 kV. Transmission electron microscopy (TEM) measurements were carried out on a Zeiss Libra 200 FE transmission electron microscope operated at 200 kV. X-ray photoelectron spectroscopy (XPS) measurements were performed on an ESCALABMK II X-ray photoelectron spectrometer using Mg as the exciting source.

2.4. Electrochemical measurements

Electrochemical measurements were performed with a CHI 660E electrochemical analyzer (CH Instruments, Inc., Shanghai) in a conventional three electrode system, using Co_3N NW/TM as working electrode, platinum wire as counter electrode and Hg/HgO and saturated calomel electrode as reference electrode in the experiment of glucose and H_2O_2, respectively. All tests were carried out at room temperature. All the potentials reported in this work were *vs.* Hg/HgO, and the equivalent relative to reversible hydrogen electrode (RHE) according to E (RHE) = E (Hg/HgO) + 0.0591 × pH + 0.9418.

3. Results and discussion

Co_3N NW/TM was obtained by low-temperature nitrogenization of $Co(CO_3)_{0.5}(OH)\cdot 0.11H_2O$ and the fabrication process is shown in Scheme 1. Fig. 1a presents the XRD pattern of the nitrogenization product and the peaks located at 39.0°, 41.6°, 44.4°, 58.2°, 70.7°, 77.7°, 85.4°, and 87.5° can be indexed to (100), (002), (101), (102), (110), (103), (112), and (201) planes of hexagonal Co_3N phase (JCPDS No. 06-0691), respectively, and other peaks can be assigned to metallic Ti (JCPDS No. 44–1294). Similarly, the diffraction peaks of $Co(CO_3)_{0.5}(OH)\cdot 0.11H_2O$ are well matched with the standard diffraction pattern of hexagonal $Co(CO_3)_{0.5}(OH)\cdot 0.11H_2O$ (JCPDS No. 48-0083) in Fig. S1. The low-magnification SEM image suggests the full coverage of $Co(CO_3)_{0.5}(OH)\cdot 0.11H_2O$ nanowire array on Ti substrate (Fig. 1b). Note that the Co_3N still maintains nanoarray feature (Fig. 1c). Energy dispersive X-ray (EDX) spectrum for the resulting nanowire verifies the presence of Co and N (Fig. 1d), and the corresponding elemental mapping analysis further indicates uniform distribution of Co and N throughout the Co_3N (Fig. 1e). High-resolution TEM (HRTEM) image (Fig. 1g) taken from such Co_3N nanowire (Fig. 1f) reveals well-resolved lattice fringes with an interplanar distance of 0.204 nm indexed to the (101) plane of Co_3N.

Fig. 1h and i presents the XPS spectra to analyse the surface electronic state and the composition of Co_3N. In the Co 2p region (Fig. 1h), two core-level peaks located at 781.3 and 796.8 eV can arise from the binding energies (BEs) of Co $2p_{3/2}$ and Co $2p_{1/2}$, respectively [18], accompanying with two satellite peaks at 786.5 and 802.6 eV [19]. Meanwhile, the BE of Co $2p_{3/2}$ is higher than that of Co^{2+} (779.9 eV) but slightly lower than that of Co^{3+} (781.6 eV) [20], denoting the Co species of Co_3N as $Co^{\delta+}$, where $2 < \delta < 3$. The N 1 s BEs at 398.5 and 403.9 eV are attributed to metal nitride [21] and N—O bond arising from surface oxidation [22,23], respectively, as shown in Fig. 1i.

The electrocatalytic activity of Co_3N NW/TM electrode for glucose oxidation was investigated using a typical three-electrode setup in 0.1 M NaOH with a scan rate of 50 mV s^{-1}. Fig. 2a shows the cyclic voltammograms (CVs) of Co_3N NW/TM and bare TM in 0.1 M NaOH in the absence and presence of 1 mM glucose with the applied potential range from 0 to 0.8 V. Bare TM shows no redox peak in the absence of glucose (curve 1), while Co_3N NW/TM displays two pairs of redox peaks (curve 3). The redox peaks at 0.32 and 0.20 V can be assigned to the Co^{2+}/Co^{3+} redox pair, and the other peaks at 0.64

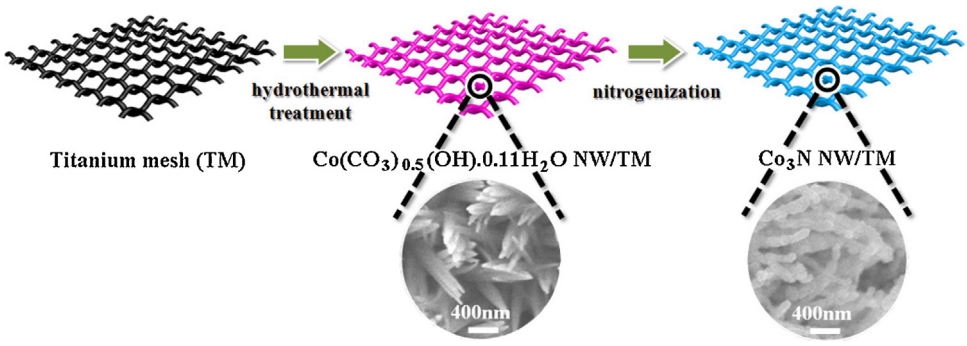

Scheme 1. A schematic diagram illustrating the fabrication process of Co_3N NW/TM.

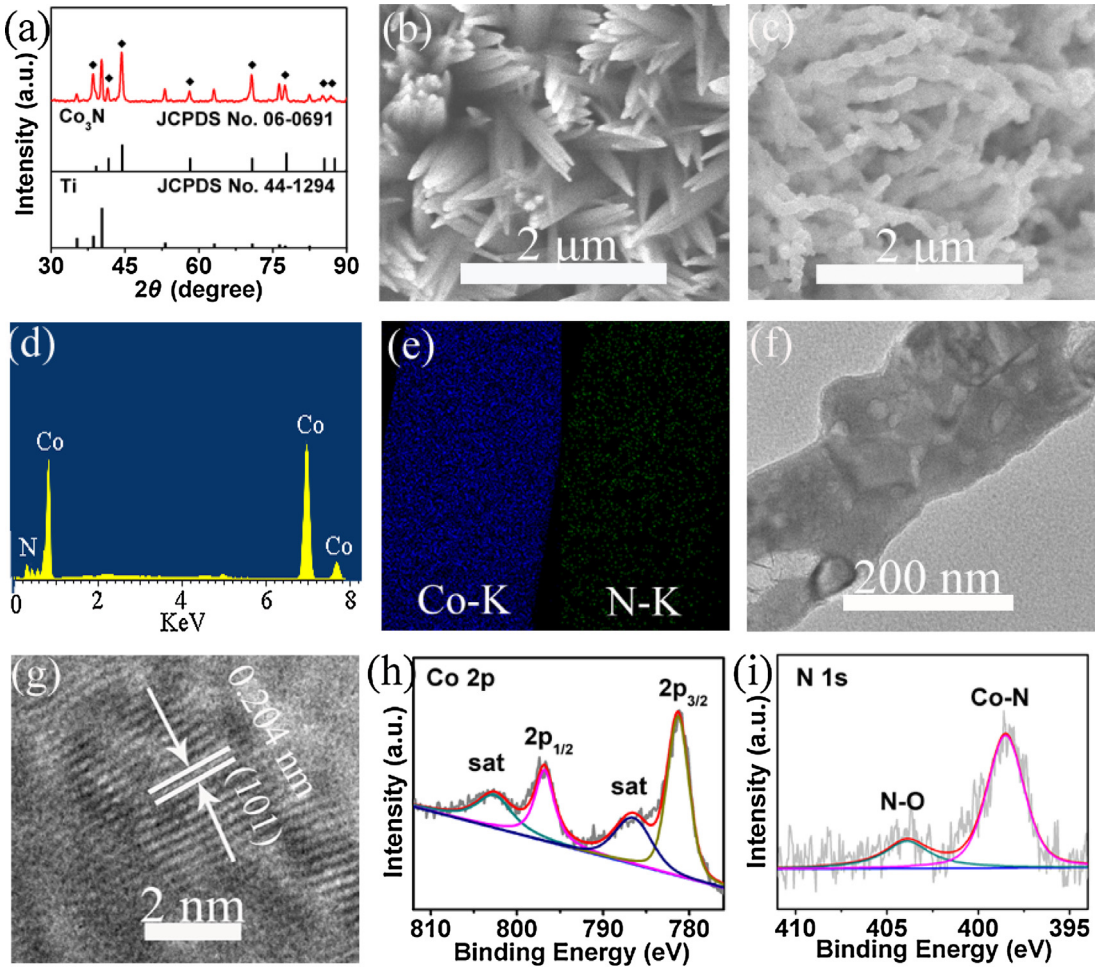

Fig. 1. (a) XRD pattern for Co_3N NW/TM. SEM images of (b) $Co(CO_3)_{0.5}(OH)\cdot 0.11H_2O$ NW/TM and (c) Co_3N NW/TM. (d) EDX spectrum for Co_3N NW/TM. (e) EDX elemental mapping images of Co and N for Co_3N NW/TM. (f) TEM image of a single Co_3N nanowire. (g) HRTEM pattern taken from Co_3N nanowire. XPS spectra in the (h) Co 2p and (i) N 1s regions for Co_3N.

and 0.55 V can attributed to the Co^{3+}/Co^{4+} pair. According to the XPS analysis, the redox mechanism of Co_3N NW/TM in NaOH solution is very similar to that of Co_3O_4, which can be described as follows [24,25]:

$$Co^{\delta+} + nOH^- + H_2O \leftrightarrow CoOOH + ne^- \quad (1)$$

$$CoOOH + H_2O \leftrightarrow Co^{4+} + 3OH + e^- \quad (2)$$

After adding 1 mM glucose, bare TM shows negligible current change, suggesting it has no catalytic activity for glucose oxidation. By contrast, Co_3N NW/TM displays a higher anodic peak current than the absence of glucose (curve 4), indicating that it is efficient for glucose electrooxidation. According to the previous reports, the electrochemical process of Co_3N NW/TM toward glucose oxidation can be explained as follows [26]:

$$Co_3N + \text{glucose} \rightarrow CoOOH + \text{glucolactone} + H_2O \quad (3)$$

The CV curves of Co_3N NW/TM in 0.1 M NaOH with 1 mM glucose were collected at various scan rates from 5 to 200 mV s^{-1} (Fig. 2b). As the scan rate increases, the separation between the oxidation and reduction peak potential for Co_3N NW/TM increases continuously, suggesting a quasi-reversible process [27,28]. The corresponding regression curve demonstrates that both anodic and

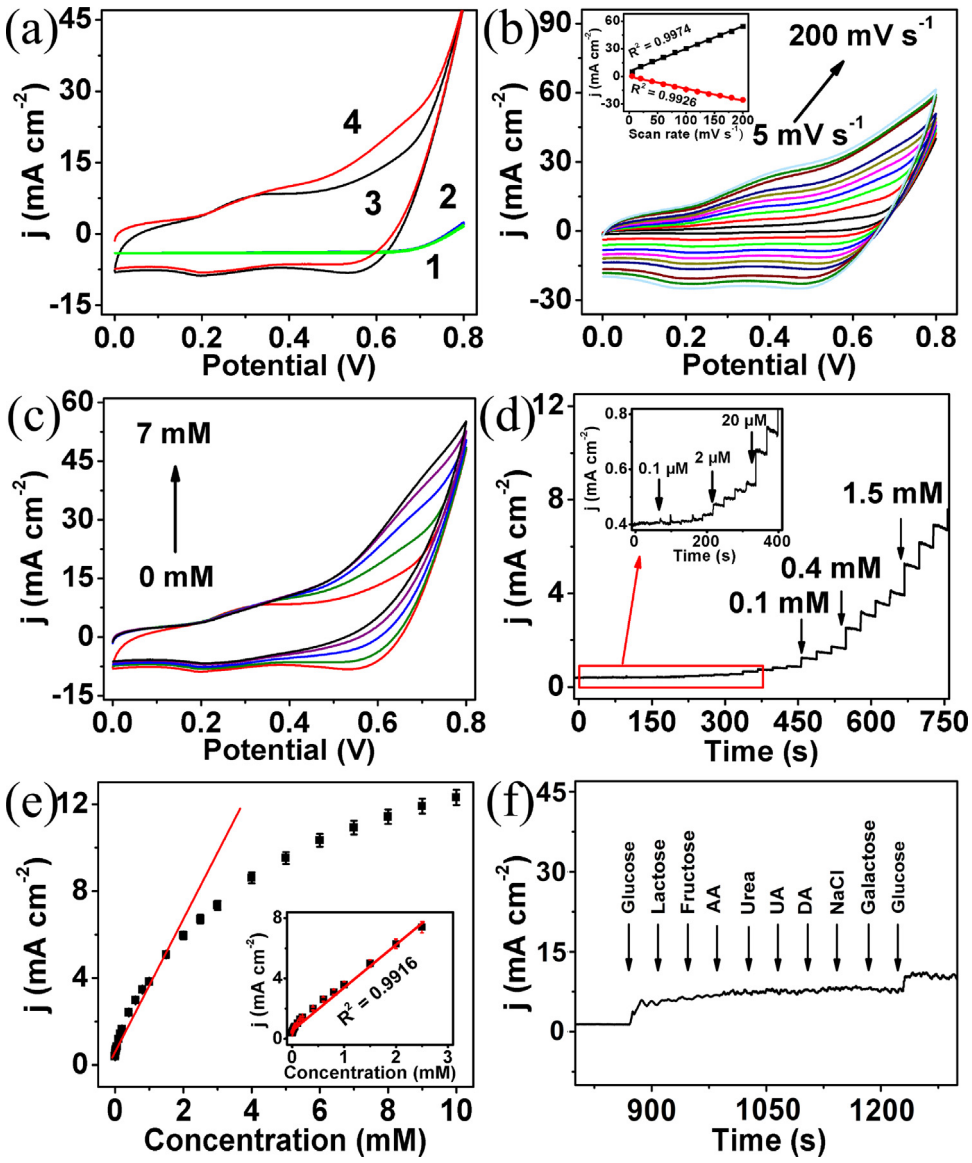

Fig. 2. (a) CVs of bare TM (curve 1 and 2) and Co_3N NW/TM (curve 3 and 4) in 0.1 M NaOH in the absence and presence of 1 mM glucose (scan rate: 50 mV s^{-1}). (b) CVs for Co_3N NW/TM in 1 mM glucose at scan rates from 5 to 200 mV s^{-1}. Inset: the corresponding plots of current density *vs.* the scan rates. (c) CVs for Co_3N NW/TM in 0.1 M NaOH in the presence of varied glucose concentrations: 0, 1, 3, 5, and 7 mM (scan rate: 50 mV s^{-1}). (d) Amperometric response of Co_3N NW/TM with successive addition of glucose in 0.1 M NaOH (inset: the current response of electrode toward the addition of glucose from 0.1 to 30 μM). (e) Calibration curve for current response to glucose concentration at high concentration range (inset: the calibration curve for current response to glucose concentration at low concentration range). (f) Aerometric response of Co_3N NW/TM electrode toward the addition of glucose (0.5 mM) and various interfering compounds (1 mM respectively) in 0.1 M NaOH.

cathodic current densities increase linearly with the scan rates, implying a surface controlled process rather than diffusion controlled process [29]. It is well-established that such transition metal catalysts require alkaline conditions to efficiently electrocatalyze glucose oxidation and increased pH leads to an increase in anodic peak current density [30,31]. For most cases, a 0.1 M alkaline solution with pH 13 is used to ensure high catalytic current because a higher pH environment is not eco-friendly and also favors oxygen evolution reaction which interferes with glucose detection. Although real samples have near-neutral pH, these sensors still perform well for blood serum samples under alkaline conditions and thus may hold great promise to detect glucose for actual cases.

Fig. 2c shows the CVs of Co_3N NW/TM obtained at different glucose concentra- tion in 0.1 M NaOH, indicate that an increase in glucose concentration from 0 to 7 mM causes larger oxidation peak current. To find the best potential for glucose detection, the amperometric current response of Co_3N NW/TM in 0.1 M NaOH with a continuous addition of 0.5 m M glucose at different potentials (from 0.40 to 0.65 V) has been investigated. As shown in Fig. S2, there is an almost obvious current response augment with the increasing of applied potential, but the background current and noise signals are more pronounced at 0.65 V. Thus, we chose 0.60 V as the optimum potential in the following experiments. Fig. 2d represents a typical current-time plot of Co_3N NW/TM electrode in 0.1 M NaOH with consecutive step changes of glucose concentrations at the potential of 0.60 V (*vs.* Hg/HgO). The inset in Fig. 2d shows the low magnification of glucose concentration from 0.1 to 30 μM. The electrode shows a fast amperometric response and can achieve steady state current density within 5 s. This Co_3N NW/TM sensor shows the same catalytic current toward glucose after several scan (Fig. S3), suggesting its good stability.

The calibration curves of the glucose sensor (Fig. 2e) within high and low concentration range exhibit a linear range of 0.1 μM – 2.5 mM with a response sensitivity of 3325.6 μA mM^{-1} cm^{-2},

Table 1
Comparison of analytical performances for Co_3N NW/TM with other non- enzymatic glucose sensors.

Electrodes	Sensitivity ($\mu A\,mM^{-1}\,cm^{-2}$)	Linear range (mM)	LOD (μM)	Stability	Ref.
Co_3N NW/TM	3325.6	0.0001–2.5	0.05	91.5% (30 d)	This work
porous CoOOH NS	526.8	0.003–1.109	1.37	–	[10]
Co_3O_4 NWs	45.8	0.0001–1.2	0.0265	95% (35 d)	[11]
TiO_2/Co_3O_4 NA	2008.82	0–3.0	1.3396	88% (21 d)	[12]
CoP NRs/GCE	116.8	0–5.5	9	–	[25]
Fe_3N-Co_2N/CC	2273.8	0.00015–8	0.059	88.7% (30 d)	[30]
CoS@C/GCE	697	0.01–0.96	2	92.6% (14 d)	[32]
Co/ITO	1720	0.005–0.18	0.25	96.2% (30 d)	[33]
Co/graphene	4700	0.00167–0.47	0.68	–	[34]
Porous Co NBs/rGO	39.32	0.15–6.25	47.5	–	[35]
CoO acicular nanorods	571.8	0.2–3.5	0.058	–	[36]
CoOOH nanosheets	341	0.03–0.7	30.9	–	[37]
Co_3O_4/PbO_2 nanorods	460.3	0.005–1.2	0.31	–	[38]
Co_3O_4 nanofibers	1440	0.005–1.2	0.08	90% (30 d)	[39]
nanoporous Co_3O_4 NWs	300.8	0.005–0.57	5	93.2% (30 d)	[40]
Zn:Co_3O_4	193	0.005–0.62	2	70% (30 d)	[41]
Cu_3P NWs/CF	11450	0.005–1	0.32	86.9% (25 d)	[42]
g-C_3N_4-GOD/GCE	–	0.1–90	11	81% (40 d)	[43]

Table 2
Concentration of glucose in human blood serum sample measured by commercial glucometer and the as-prepared Co_3N NW/TM.

	Measured by glucometer (mM)	Determined by our sensor (mM)	Relative error (%)
Reading	10	9.8	4

and the detection limit is 50 nM at the signal-to-noise ratio of 3 (S/N = 3). These values are more superiority than those of other Co-based non-enzymatic glucose sensors [10–12,25,30,32–43] and detailed comparison is listed in Table 1. Nitrogen content in Co_3N nanowire was determined as a nearly 3:1 atomic ratio of Co to N by EDX. We also made Co_2N nanowire array by 6 h nitridation and found both catalyst electrodes show quite different catalytic performances (Fig. S4), suggesting the nitrogen content has heavy influence on the catalytic activity.

Selectivity is another major factor to assess the performance of electrode for nonenzymatic glucose detection. The influence of common interfering species such as lactose, fructose, galactose, AA, urea, UA, NaCl, and DA was also investigated. Fig. 2f shows the amperometric responses of Co_3N NW/TM toward successive addition of 0.5 mM glucose and of 1 mM other interferences in 0.1 M NaOH. It is clearly seen that Co_3N NW/TM has remarkable response toward glucose but negligible response toward interfering species and the current density increases again with another addition of glucose, indicating that the sensor is highly selective to glucose in the presence of common interfering compounds. The long-term stability of Co_3N NW/TM has also been investigated for practical application. After being exposed to air for one month in room temperature, Co_3N NW/TM keeps about 91.5% of its initial response current, suggesting a good long-term stability. The reproducibility of Co_3N NW/TM was also evaluated by measuring the cyclic voltammetry response to 1 mM glucose in 0.1 M NaOH for five Co_3N NW/TM parallel electrodes. The relative standard deviation (RSD) of the anode peak current densities is 4.3%, indicating a favourable reproducibility.

To testify the feasibility of Co_3N NW/TM in practical analysis, we employed the biosensor to measure glucose in human blood serum. Quantitative determination of glucose was analyzed by the standard addition method. The concentration of glucose in human blood serum sample measured by our electrochemical method agrees well with the certificated value obtained by commercial glucometer (Sannuo biological sensor co., LTD) and the relative error is 4%. The corresponding results are shown in Table 2, which indicated that such sensor holds great promise for real samples detection application. Moreover, the stability of Co_3N NW/TM is investigated in human blood serum at lower pH than 0.1 M NaOH. After the Co_3N NW/TM was kept in an ambient environment for a period of time, it maintained 92.4% of its initial response. And such long-term stability was not affected by solution pH.

H_2O_2 is a common reactive oxygen species [44], and play an important role in the fields of environmental protection, clinical studies, food, pharmaceutical, chemistry [45,46]. However, under overloading conditions, it may cause oxidative stress that can induce cancer, Alzheimer's disease and Parkinson's disease [47–49]. Many techniques for H_2O_2 detection, including spectrometry, titrimetry, chemiluminescence and electrochemistry, have been developed. Among them, electrochemical technique has been proven to be an inexpensive and effective way due to its intrinsic simplicity and high sensitivity and selectivity. Notably, Co_3N NW/TM exhibit remarkable catalytic activity for electrochemical detection of H_2O_2. Fig. 3a shows the CVs of bare TM and Co_3N NW/TM toward the reduction of H_2O_2 in 0.1 M phosphate buffer solution (PBS, pH = 7.4), with the potential range from 0 to −0.7 V at a scan rate of 50 mV s^{-1}. In contrast, no redox peaks were observed for bare TM in the lack H_2O_2 (curve 1), and a very weak reducibility to H_2O_2 after addition of 1 mM analyte (curve 2). Interestingly, in the absence of H_2O_2, Co_3N NW/TM shows no obvious redox peaks (curve 3) but higher current response than bare TM, and the reduction peak arise in the presence of 1 mM H_2O_2 (curve 4). All the above observations indicate that Co_3N NW/TM exhibits an excellent catalytic performance for H2O2 reduction, and the large catalytic current obtained could be attributed to Co_3N NW/TM. Fig. 3b presents the CVs of Co_3N NW/TM with different scan rates ranging from 5 to 200 mV s^{-1}. The good linear relationship between the cathodic current and scan rates implies a surface controlled process of H_2O_2 reduction on the Co_3N NW/TM electrode [29].

The electrochemical performance of Co_3N NW/TM electrode towards different concentrations of H_2O_2 in 0.1 M PBS was studied employing amperometric measurements, as shown in Fig. 3c. The reduction peak current increases gradually with increased concentrations of H_2O_2. To determine the optimum applied potential, we studied the amperometric current response of Co_3N NW/TM in 0.1 M PBS with continuous addition of 1 mM H_2O_2 at different potentials from −0.10 to −0.30 V (Fig. S5). A remarkable increase in current response could be observed with increasing applied potential from −0.10 to −0.20 V, but decreases from −0.20 to −0.30 V. Therefore, we chose −0.20 V as the optimum potential in following experiments. Fig. 3d shows the typical amperometric responses of Co_3N NW/TM to the consecutive addition of H_2O_2 in 0.1 M PBS at −0.20 V. The fabricated electrode exhibits a fast amperometric

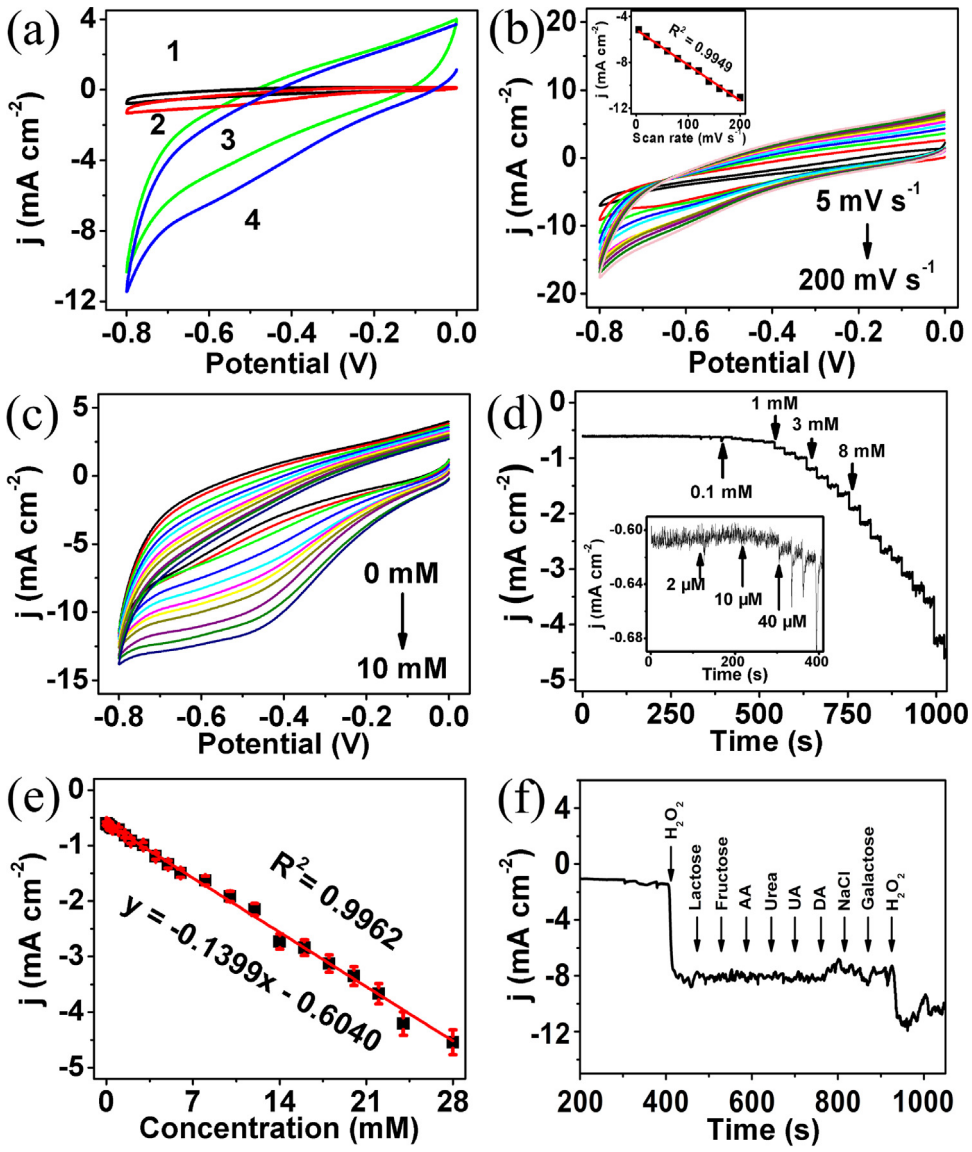

Fig. 3. CVs of bare TM (curve 1 and 2) and Co_3N NW/TM (curve 3 and 4) in 0.1 M PBS in the absence (curve 1 and 3) and presence (curve 2 and 4) of 1 mM H_2O_2 (scan rate: 50 mV s^{-1}). (b) CVs for Co_3N NW/TM in 1 mM H_2O_2 at scan rates from 5 to 200 mV s^{-1}. Inset: the corresponding plots of current density *vs.* the scan rates. (c) CVs for Co_3N NW/TM in 0.1 M NaOH in the presence of varied H_2O_2 (scan rate: 50 mV s^{-1}). (d) Amperometric response of Co_3N NW/TM with successive addition of H_2O_2 in 0.1 M PBS (inset: the current response of electrode toward the addition of glucose from 2 to 80 μM). (e) Calibration curve for current response to H_2O_2 concentration at high concentration range (inset: the calibration curve for current response to H_2O_2 concentration at low concentration range). (f) Amperometric response of Co_3N NW/TM electrode toward the addition of H_2O_2 (1 mM) and various interfering compounds (10 mM respectively) in 0.1 M PBS.

Table 3
Comparison of analytical performances of Co_3N NW/TM with other Co- based electrochemical H_2O_2 sensors.

Electrodes	Sensitivity (μA mM^{-1} cm^{-2})	Linear range (mM)	LOD (μM)	Stability	Ref.
Co_3N NW/TM	139.9	0.002–28	1	92.1% (30 d)	This work
Fe_3N-Co_2N/CC	2273.8	0.00015–8	0.059	90.2% (30 d)	[30]
RGO-Pt/GCE	459	0.5–3.47	~0.2	~81% (14 d)	[43]
CoS	17.4	0.005–14.82	1.5	–	[50]
3D N-Co-CNT@NG	28.66	0.002–7.449	2	–	[51]
Co_3O_4/MWCNTs	1000	0.02–0.43	2.46	–	[52]
CoTPP/RGO	4.2	0.0001–2.4	0.03	–	[53]
PPy-Co NCs	103.48	0.02–1	2.05	–	[54]
CuO-SiNWs/GCE	22.27	0.01–13.18	1.6	81.6% (14 d)	[55]
AgNP-TiO_2 NWs	–	0.1–60	1.70	89% (30 d)	[56]
CoP NWs	–	0.001–12	0.48	90.2% (30 d)	[57]

response toward H_2O_2 and reaches a steady-state density within 5 s. Note that oxygen interferes with H_2O_2 detection (Fig. S6). The H_2O_2 sensor demonstrates a linear range of 2 Mμ – 28 mM, a response sensitivity of 139.9 μA mM^{-1} cm^{-2}, and a detection limit of 1 μM (S/N = 3), shows in Fig. 3e. These parameters are correspondingly superior to a number of Co-based non-enzymatic H_2O_2

sensors [30,43,50–57] (Table 3 shows the deteailed comparison). Although hierarchical 3D N-Co-CNT@NG is also efficient for such sensing [51], the fabrication of our Co_3N NW/TM is less energy-intensive with lower annealing temperature and easy to scale-up for mass production. Moreover, the Co_3N nanoarray can be developed on any conductive substrates.

The anti-interference experiment is investigated to evaluate the selectivity of the proposed H_2O_2 biosensor. In Fig. 3f, we can observe a remarkable response towards H_2O_2, while the current response is insignificant with the addition of 10 mM lactose, fructose, AA, urea, UA, NaCl, DA and galactose in the same sample, indicating the good selectivity of Co_3N NW/TM for H_2O_2. Reproducibility tests were carried out by employing five different electrodes fabricated under 0.1 M PBS containing 1 mM H_2O_2. The RSD of about 5.2% was obtained, which indicates that the fabrication methodology of the sensors results in acceptable reproducibility. After being exposed to air for one month at room temperature, the Co_3N NW/TM shows about 92.1% of its initial response current.

4. Conclusions

In summary, Co_3N NW/CF has been proven as an efficient catalyst electrode for glucose oxidation and H_2O_2 reduction under alkaline and neutral conditions, respectively. As a non-enzymatic electrochemical sensor, it shows high sensitivity and selectivity with satisfactory stability and reproducibility. This study not only provides an attractive low-cost easily made electrode material for high-efficiency glucose and H_2O_2 detection, but would open new opportunity to develop the use of a 3D metal nitrides nanoarray as superb sensors for analytical applications.

Appendix A. Supplementary data

Supplementary data associated with this article can be found, in the online version, at http://dx.doi.org/10.1016/j.snb.2017.08.098.

References

[1] A. Pandey, P. Tripathi, R. Pandey, R. Srivatava, S. Goswami, Alternative therapies useful in the management of diabetes: a systematic review, J. Pharm. Bioallied Sci. 3 (2011) 504–512.
[2] M. Gourzi, A. Rouane, R. Guelaz, M.S. Alavi, M.B. McHugh, M. Nadi, P. Roth, Non-invasive glycaemia blood measurements by electromagnetic sensor: study in static and dynamic blood circulation, J. Med. Eng. Technol. 29 (2009) 22–26.
[3] C.D. Malchoff, K. Shoukri, J.I. Landau, J.M. Buchert, A novel noninvasive blood glucose monitor, Diabetes Care 25 (2002) 2268–2275.
[4] R. Hu, A.C. Stevenson, C.R. Lowe, An acoustic glucose sensor, Biosens. Bioelectron. 35 (2012) 425–428.
[5] M.S. Steiner, A. Duerkop, O.S. Wolfbeis, Optical methods for sensing glucose, Chem. Soc. Rev. 40 (2011) 4805–4839.
[6] J. Wang, Electrochemical glucose biosensors, Chem. Rev. 108 (2012) 814–825.
[7] C. L Jr., C. Lyons, Electrode systems for continuous monitoring in cardiovascular surgery, Ann. N. Y. Acad. Sci. 102 (2010) 29–45.
[8] S. Park, H. Boo, T.D. Chung, Electrochemical non-enzymatic glucose sensors, Anal. Chim. Acta 556 (2006) 46–57.
[9] X. Niu, X. Li, J. Pan, Y. He, F. Qiu, R. Yan, Recent advances in non-enzymatic electrochemical glucose sensors based on non-precious transition metal materials: opportunities and challenges, RSC Adv. 6 (2016) 84893–84905.
[10] L. Zhang, C. Yang, G. Zhao, J. Mu, Y. Wang, Self-supported porous CoOOH nanosheet arrays as a non-enzymatic glucose sensor with good reproducibility, Sens. Actuators B 210 (2015) 190–196.
[11] Y. Xu, Cao, Y. Chen, W. Huang, D. Chen, Q. Huang, J. Tu, Self-supported porous CoOOH nanosheet arrays as a non-enzymatic glucose sensor with good reproducibility, Eur. J. Inorg. Chem. 2016 (2016) 3163–3168.
[12] K. Khun, Z.H. Ibupoto, X. Liu, V. Beni, M. Willander, The ethylene glycol template assisted hydrothermal synthesis of Co_3O_4 nanowires; structural characterization and their application as glucose non-enzymatic sensor, Mater. Sci. Eng. B 194 (2015) 94–100.
[13] Z. Gao, L. Zhang, C. Ma, Q. Zhou, Y. Tang, Z. Tu, W. Yang, L. Cui, Y. Li, TiO_2 decorated Co_3O_4 acicular nanotube arrays and its application as a non-enzymatic glucose sensor, Biosens. Bioelectron. 80 (2016) 511–518.
[14] J. Tian, Q. Liu, A.M. Asiri, X. Sun, Self-supported nanoporous cobalt phosphide nanowire arrays: an efficient 3D hydrogen-evolving cathode over the wide range of pH 0–14, J. Am. Chem. Soc. 136 (2014) 7587–7590.
[15] C. Tang, N. Chen, Z. Pu, W. Xing, X. Sun, NiSe nanowire film supported on nickel foam: an efficient and stable 3D bifunctional electrode for full water splitting, Angew. Chem. Int. Ed. 54 (2015) 9351–9355.
[16] P. Jiang, Q. Liu, Y. Liang, J. Tian, A.M. Asiri, X. Sun, A cost-effective 3D hydrogen evolution cathode with high catalytic activity: feP nanowire array as the active phase, Angew. Chem. Int. Ed. 53 (2014) 12855–12859.
[17] P. Chen, K. Xu, T. Yun, X. Li, S. Tao, Z. Fang, W. Chu, X. Wu, C. Wu, Cobalt nitrides as a class of metallic electrocatalysts for the oxygen evolution reaction, Inorg. Chem. Front. 3 (2016) 236–242.
[18] Z. Yao, X. Zhang, F. Peng, H. Yu, H. Wang, J. Yang, Novel highly efficient alumina-supported cobalt nitride catalyst for preferential CO oxidation at high temperatures, Int. J. Hydrogen Energy 36 (2011) 1955–1959.
[19] Y. Zhang, B. Ouyang, J. Xu, G. Jia, S. Chen, R.S. Rawat, H. Fan, Rapid synthesis of cobalt nitride nanowires: highly efficient and low-cost catalysts for oxygen evolution, Angew. Chem. Int. Ed. 55 (2016) 8670–8674.
[20] K. Hada, A.M. Nagai, S. Omi, Characterization and HDS activity of cobalt molybdenum nitrides, J. Phys. Chem. B 105 (2001) 217–219.
[21] Y.L. Leung, P.C. Wong, K.A.R. Mitchell, K.J. Smith, X-ray photoelectron spectroscopy studies of the reduction of MoO thin films by NH_3, Appl. Surf. Sci. 136 (1998) 147–158.
[22] Y. Wang, D. Liu, Z. Liu, C. Xie, J. Huo, S. Wang, Porous cobalt-iron nitride nanowires as excellent bifunctional electrocatalysts for overall water splitting, Chem. Commun. 52 (2016) 12614–12617.
[23] Z. Wang, W. Cai, X. Hong, X. Zhao, F. Xu, C. Cai, Photocatalytic degradation of phenol in aqueous nitrogen-doped TiO_2 suspensions with various light sources, Appl. Catal. B Environ. 57 (2005) 223–231.
[24] C. Barbero, G.A. Planes, M.C. Miras, Redox coupled ion exchange in cobalt oxide films, Electrochem. Commun. 3 (2001) 113–116.
[25] Q. Sun, M. Wang, S. Bao, Y. Wang, S. Gu, Analysis of cobalt phosphide (CoP) nanorods designed for non-enzyme glucose detection, Analyst 141 (2015) 256–260.
[26] Y. Ding, Y. Wang, L. Su, M. Bellagamba, H. Zhang, Y. Lei, Electrospun Co_3O_4 nanofibers for sensitive and selective glucose detection, Biosens. Bioelectron. 26 (2010) 542–548.
[27] M. Tyagi, M. Tomar, V. Gupta, Glad assisted synthesis of NiO nanorods for realization of enzymatic reagentless urea biosensor, Biosen. Bioelectron. 52 (2014) 196–201.
[28] Z. Matharu, P. Pandey, M. Pandey, Functionalized gold nanoparticles-octadecylamine hybrid langmuir-blodgett film for enzyme sensor, Electroanalysis 21 (2010) 1587–1596.
[29] R. Zhang, J. Ma, W. Wang, B. Wang, R. Li, Zeolite-encapsulated M(Co, Fe, Mn)(SALEN) complexes modified glassy carbon electrodes and their application in oxygen reduction, J. Electroanal. Chem. 643 (2010) 31–38.
[30] D. Zhou, X. Cao, Z. Wang, S. Hao, X. Hou, F. Qu, X. Sun, Fe_3N-Co_2N nanowires array: a non-noble-metal bifunctional catalyst electrode for high-performance glucose oxidation and H_2O_2 reduction toward non-enzymatic sensing application, Chem. Eur. J. 23 (2017) 5214–5218.
[31] Z. Wang, X. Cao, D. Liu, S. Hao, G. Du, X. Sun, Ternary NiCoP nanosheet array on a Ti mesh: a high-performance electrochemical sensor for glucose detection, Chem. Commun. 52 (2016) 14438–14441.
[32] P. Qu, Z. Gong, H. Cheng, W. Xiong, X. Wu, P. Pei, R. Zhao, Y. Zeng, Z. Zhu, Nanoflower-like CoS-decorated 3D porous carbon skeleton derived from rose for a high performance nonenzymatic glucose sensor, RSC Adv. 5 (2015) 106661–106667.
[33] T. Wang, Y. Yu, H. Tian, J. Hu, A novel non-enzymatic glucose sensor based on cobalt nanoparticles implantation-modified indium tin oxide electrode, Electroanalysis 26 (2014) 2693–2700.
[34] S. Ci, Z. Wen, S. Mao, Y. Hou, S. Cui, Z. He, J. Chen, One-pot synthesis of high-performance Co/graphene electrocatalysts for glucose fuel cells free of enzymes and precious metals, Chem. Commun. 51 (2015) 9354–9357.
[35] Y. Song, C. Wei, J. He, X. Li, X. Lu, L. Wang, Porous Co nanobeads/rGO nanocomposites derived from rGO/Co-metal organic frameworks for glucose sensing, Sens. Actuators B. Chem. 220 (2015) 1056–1063.
[36] C. Kung, C. Lin, Y. Lai, R. Vittal, K. Ho, Cobalt oxide acicular nanorods with high sensitivity for the non-enzymatic detection of glucose, Biosens. Bioelectron. 27 (2011) 125–131.
[37] K.K. Lee, P.Y. Loh, C.H. Sow, W.S. Chin, CoOOH nanosheets on cobalt substrate as a non-enzymatic glucose sensor, Electrochem. Comm. 20 (2012) 128–132.
[38] T. Chen, X. Li, C. Qiu, W. Zhu, H. Ma, S. Chen, O. Meng, Electrochemical sensing of glucose by carbon cloth-supported Co_3O_4/PbO_2 core-shell nanorod arrays, Biosens. Bioelectron. 53 (2014) 200–206.
[39] C. Guo, X. Zhang, H. Huo, C. Xu, X. Han, Co_3O_4 microspheres with free-standing nanofibers for high performance non-enzymatic glucose sensor, Analyst 138 (2013) 6727–6731.
[40] L. Kang, D. He, L. Bie, P. Jiang, Nanoporous cobalt oxide nanowires for non-enzymatic electrochemical glucose detection, Sens. Actuators B Chem. 220 (2015) 888–894.
[41] M. Chowdhury, F. Cummings, M. Kebede, V. Fester, Binderless solution processed Zn doped Co3O4 film on FTO for rapid and selective non-enzymatic glucose detection, Electroanalysis 29 (2016) 578–586.
[42] L. Xie, A.M. Asiri, X. Sun, Monolithically integrated copper phosphide nanowire: an efficient electrocatalyst for sensitive and selective nonenzymatic glucose detection, Sens. Actuators B Chem. 244 (2017) 11–16.

[43] J. Tian, Q. Liu, C. Ge, Z. Xing, A.M. Asiri, A.O. Al-Youbi, X. Sun, Ultrathin graphitic carbon nitride nanosheets: a low-cost, green, and highly efficient electrocatalyst toward the reduction of hydrogen peroxide and its glucose biosensing application, Nanoscale 5 (2013) 8921–8924.
[44] Y. Zhang, X. Bai, X. Wang, K.K. Shiu, Y. Zhu, H. Jiang, Highly sensitive graphene-Pt nanocomposites amperometric biosensor and its application in living cell H_2O_2 detection, Anal. Chem. 86 (2014) 9459–9465.
[45] X. Shu, Y. Chen, H. Yuan, S. Gao, D. Xiao, H_2O_2 sensor based on the room-temperature phosphorescence of nano TiO_2/SiO_2 composite, Anal. Chem. 79 (2007) 3695–3702.
[46] W. Chen, S. Cai, Q. Ren, W. Wen, Y. Zhao, Recent advances in electrochemical sensing for hydrogen peroxide: a review, Analyst 137 (2011) 49–58.
[47] D. Trachootham, J. Alexandre, P. Huang, Targeting cancer cells by ROS-mediated mechanisms: a radical therapeutic approach, Nat. Rev. Drug Discov. 8 (2009) 579–591.
[48] Y. Wei, Y. Zhang, Z. Liu, M. Guo, A novel profluorescent probe for detecting oxidative stress induced by metal and H_2O_2 in living cells, Chem. Commun. 46 (2010) 4472–4474.
[49] A. Sevanian, P. Hochstein, Mechanisms and consequences of lipid peroxide in biological systems, Ann. Rev. Nutr. 5 (1985) 365–390.
[50] W. Wu, B. Yu, H. Wu, S. Wang, Q. Xia, Y. Ding, Synthesis of tremella-like CoS and its application in sensing of hydrogen peroxide and glucose, Mater. Sci. Eng. C Mater. Biol. Appl. 70 (2017) 430–437.
[51] J. Balamurugan, T.D. Thanha, G. Karthikeyana, N.H. Kima, J.H. Lee, A novel hierarchical 3D N-Co-CNT@NG nanocomposite electrode for non-enzymatic glucose and hydrogen peroxide sensing applications, Biosens. Bioelectron. 89 (2016) 970–977.
[52] H. Heli, J. Pishahang, Cobalt oxide nanoparticles anchored to multiwalled carbon nanotubes: synthesis and application for enhanced electrocatalytic reaction and highly sensitive nonenzymatic detection of hydrogen peroxide, Electrochim. Acta 123 (2014) 518–526.
[53] L. Zheng, D. Ye, L. Xiong, J. Xu, K. Tao, Z. Zou, D. Huang, X. Kang, S. Yang, J. Xia, Preparation of cobalt-tetraphenylporphyrin/reduced graphene oxide nanocomposite and its application on hydrogen peroxide biosensor, Anal. Chim. Acta 768 (2013) 69–75.
[54] T. Marimuthu, M.R. Mahmoudian, S. Mohamad, Y. Alias, Synthesis and characterization of non-enzymatic hydrogen peroxide sensor of polypyrrole coated cobalt nanocomposites, Sens. Actuators B Chem. 202 (2014) 1037–1043.
[55] J. Huang, Y. Zhu, H. Zhong, X. Yang, C. Li, Dispersed CuO nanoparticles on a silicon nanowire for improved performance of nonenzymatic H_2O_2 detection, ACS Appl. Mater. Interface 6 (2014) 7055.
[56] X. Qin, W. Lu, Y. Luo, G. Chang, M.A. Abdullah, X. Sun, Green photocatalytic synthesis of Ag nanoparticle-decorated TiO_2 nanowires for nonenzymatic amperometric H_2O_2, detection, Electrochim. Acta 74 (2012) 275–279.
[57] D. Liu, T. Chen, W. Zhu, L. Cui, A.M. Asiri, X. Sun, Cobalt phosphide nanowires: an efficient electrocatalyst for enzymeless hydrogen peroxide detection, Nanotechnology 27 (2016), 33T01.

Biographies

Fengyu Xie obtained her PhD degree in materials science and engineering form Chongqing University in 2013. She as a postdoctoral fellow worked in College of Microelectronics and Solid-State Electronics in Electronic Science and Technology University from 2014 till now. She is a lecturership in College of Chemistry and Materials Science at Sichuan Normal University. Her research interests focus on electrochemical and optical sensing.

Xiaoqin Cao received her BS degree in Pharmacy (2015) from Chengdu University of Traditional Chinese Medicine. She is now pursuing her MS study at Southwest Jiaotong University under supervision of Prof. Qun Lu. In 2006, she did research at Sichuan University under the supervision of Prof. Xuping Sun. Her current research focuses on developing medicinal chemistry.

Fengli Qu obtained her PhD degree in Analytical Chemistry in Hunan University (China) in 2008. She worked in LCPME-CNRS (Nancy, France) as a postdoctoral fellow from 2008 to 2009 and as a Visiting Professor in Princeton University (Princeton, USA) from 2013 to 2014. Currently, she is a Professor in College of Chemistry and Chemical Engineering at Qufu Normal University. Her research interests include nanomaterial applications and biosensor development.

Abdullah M. Asiri received his PhD from University of Wales, College of Cardiff, UK in 1995. He is the Head of the Chemistry Department at King Abdulaziz University since October 2009 and he is the founder and the Director of the Center of Excellence for Advanced Materials Research. He is a Professor of Organic Photochemistry. He holds three USA patents, more than 820 Publications in international Journals, four book Chapters, and 14 Books.

Xuping Sun received his PhD degree in Chemistry from Changchun Institute of Applied Chemistry under supervision of Prof. Erkang Wang in 2005. His PhD thesis was awarded for National Excellent Hundred Doctoral Dissertation in 2008. He was an Alexander von Humboldt Fellow at Konstanz University, a postdoctoral research associate at Toronto University and Purdue University. He is now a professor at Sichuan University. He is also an adjunct professor at China West Normal University King Abdulaziz University. He has authored or co-authored over 340 papers in peer-reviewed journals with total citation over 13000 times and H-index of 67. His research focuses on the design and development of multifunctional nanostructures for sensing and energy-related applications.